A Comparison of the Mechanical Properties and Microstructures of Intermetallic Matrix Composites Fabricated by Two Different Methods

REBECCA A. MacKAY, SUSAN L. DRAPER, ANN M. RITTER, and PAUL A. SIEMERS

The tensile properties of SCS-6 SiC fiber-reinforced Ti-24Al-11Nb (at. pct) have been measured over the past several years by a number of investigators. These composites have been fabricated by different techniques and tend to exhibit a large amount of scatter in the longitudinal tensile properties. To date, it is not known if one optimized fabrication method provides composites with improved mechanical properties over those produced by other optimized methods, since carefully controlled experiments have not been performed to determine this. Thus, the purpose of the present study was to compare the longitudinal tensile strengths of SCS-6 SiC/Ti-24Al-11Nb composites that had been fabricated by the powder-cloth method and the low-pressure plasma spray (LPPS) method. In this study, the same lots of matrix powder and reinforcing fiber were used for fabricating the composites. It was determined that the powder-cloth and plasma spray methods produced composites having very similar tensile properties. Both fabrication methods induced damage in a small percentage of fibers, which manifested itself in the form of bimodal Weibull distributions of extracted fiber strengths. It appeared that the particular lot of SCS-6 fiber used in fabricating both types of composites was more susceptible to fabrication damage than those used in previous studies. This article also shows the dramatic effect that different handling and testing techniques can have on measured fiber strengths.

I. INTRODUCTION

THE tensile properties of SCS-6 SiC fiber-reinforced Ti-24Al-11Nb (at. pct) have been measured by a number of investigators.[1–7] The SiC/Ti-24Al-11Nb composites studied in these investigations have been fabricated by different techniques such as the powder-cloth,[1,2,3] foil-fiber-foil,[1,4,5] low-pressure plasma spray (LPPS),[1,5,6] and wire-arc spray[1,7] methods. Unidirectional SiC/Ti-24Al-11Nb composites tend to exhibit a large amount of scatter in the longitudinal tensile properties at ambient temperature. For example, the longitudinal ultimate tensile strength (UTS) at ambient temperature has been reported[1] to range from about 840 to 1500 MPa in powder-cloth composites and from about 900 to 2010 MPa in low-pressure plasma-sprayed composites, when random fiber lots were used during fabrication. A similar range in properties has been observed in composites fabricated by other techniques.

Because of the wide range in these composite strengths, it has been difficult to determine if a particular fabrication method produces composites with improved mechanical properties. In fact, direct composite property comparisons between different studies in the literature can sometimes lead to erroneous conclusions, since fabrication methods are being optimized continually. Another complication that hampers these cross comparisons is that the starting fiber and matrix materials in these studies are from different lots. Thus, differences in composite properties between studies cannot necessarily be attributed to different fabrication methods but may actually be the result of differences in starting fiber and/or matrix quality. Draper *et al.*[2] have shown that when the variability in as-received fiber strength is reduced in a given SiC/Ti-24Al-11Nb composite panel, the scatter in composite strength is reduced, since the longitudinal strength of unidirectional composites is controlled primarily by the fibers.

Thus, the purpose of the present study was to compare the longitudinal tensile strengths of unidirectional SCS-6 SiC/Ti-24Al-11Nb composites that have been fabricated by two different methods, the powder-cloth technique and the LPPS technique. The powder-cloth technique has been used extensively at the NASA-Lewis Research Center and has been optimized for SiC/Ti-24Al-11Nb. The LPPS process has been developed and optimized for SiC/Ti-24Al-11Nb at the General Electric Corporate Research and Development Center. It is believed that this is the first study of its kind to make such a comparison between fabrication methods in a carefully controlled series of experiments. Both processes used matrix powder and reinforcing fiber from the same lots of material. In this way, any differences in the mechanical properties of the composites could be attributed directly to the fabrication method, since the starting constituent materials were the same. SCS-6 fiber of known strength was incorporated into the composites, and the effect of processing on the as-received fiber strength was determined by extracting the fiber from the as-fabricated composite panels. Extensive fiber testing and detailed Weibull analyses were conducted so that the composite strengths could be rationalized. In addition, the microstructures of the composites after fabrication

REBECCA A. MacKAY, Senior Materials Scientist, and SUSAN L. DRAPER, Materials Research Engineer, are with the NASA-Lewis Research Center, Cleveland, OH. ANN M. RITTER, Staff Metallurgist, and PAUL A. SIEMERS, Staff Chemist, are with General Electric Company, Corporate Research and Development, Schenectady, NY.

Manuscript submitted October 6, 1993.

and after tensile testing were examined and related to possible failure mechanisms.

II. MATERIALS AND PROCEDURES

The composites used in this study were fabricated by the powder-cloth process[1,8] and the LPPS process.[1,5,9] The same lot of −60/+80 mesh matrix powder and the same lot of fiber were used for each fabrication process. The prealloyed PREP® powder had a nominal composition of Ti-24Al-11Nb (at. pct). The fiber used was the 142 μm diameter SCS-6[10] SiC fiber, which was purchased in 1989 from Textron Specialty Materials, Lowell, MA.

In the powder-cloth process, the matrix powder was blended with a binder, and the mixture was rolled into thin sheets. The fiber mat preforms were made by winding a continuous length of SCS-6 fiber at a spacing of 50 fibers/cm onto a drum, which was then coated with a binder. The powder cloths and fiber mats were cut to size, stacked in alternating layers, and consolidated by vacuum hot pressing. The targeted volume fraction of fiber in the consolidated composite was 25 vol pct. Four unidirectional composite plates, each with four plies of fiber, were made using this technique; each plate measured 5 × 15 cm, with the latter dimension being the fiber direction. Each composite panel was fabricated using fiber from a single-drum winding, except for the fourth powder-cloth panel (91086-4), which incorporated two plies from each of the first two windings. Approximately 2.5 m of fiber were removed from the spool before and after each drum winding for subsequent tensile testing. In this way, the as-received fiber strength in each winding was bracketed, and any changes in fiber strength along the spool could be traced.

In the LPPS process, molten drops of the matrix powder were sprayed onto a single ply of the SCS-6 fibers, which was also wound at a spacing of 50 fibers/cm on a drum. The as-sprayed monotapes were cut to size, stacked, and consolidated by hot isostatic pressing (HIPing). The targeted volume fraction of fiber in the consolidated composite was 25 vol pct. Four unidirectional composite plates, each with four plies of fiber, were fabricated by this method; each plate measured 10 × 12.7 cm, with the latter dimension being the fiber direction. Each panel was fabricated using fiber from a single winding. Fiber was set aside before and after each drum winding, so that the as-received strength of the fiber could be evaluated for each composite panel.

Reduced gage specimens were machined from the powder-cloth and the plasma-sprayed composites by diamond cutting and diamond grinding; these specimens had a 114.3 mm total length, a 25.4 mm gage length, a 6.35 mm gage width, and a nominal 1.3 mm thickness. Rectangular specimens, 114.3 mm long by 10.2 mm wide, were also machined from the plasma-sprayed panels. Specimen broad surfaces were ground with 180- and 600-grit SiC paper to remove the 0.010 mm surface reaction that often formed during consolidation. The specimens were tensile tested at room temperature in air at a constant crosshead speed of 0.008 mm/s. Strain was measured with an axial extensometer attached to the edges of the specimen by a 100-gm spring force.

A fiber extraction procedure was performed to retrieve fiber from the as-fabricated composite plates. This procedure consisted of etching the matrix away in a solution of 85 pct H_2O, 10 pct HF, and 5 pct HNO_3 for 7 hours at room temperature. The etching solution was changed every hour, and the fibers were rinsed in water and dried at room temperature after the etching was completed. Some as-received fibers were also placed in this etching solution to determine if the etchant exposure itself had any influence on the fiber strength. Extensive single-fiber tensile testing was performed to characterize the extracted fibers, the etched fibers, and the as-received fibers. These fiber tests were conducted at room temperature in air at a constant crosshead speed of 0.042 mm/s. At NASA-Lewis, fibers with an 88.9 mm total length were mounted for testing on cardboard tabs with cyanoacrylate glue and adhesive tape, producing a gage length of 12.7 mm; this procedure was followed for the as-received fibers, the etched fibers, and the fibers that were extracted from the powder-cloth panels. Two variations in the fiber testing method were used at the General Electric Laboratory: as-received fibers with a 25.4 mm gage length were tested without the use of cardboard tabs, by placing loose sheets of filter paper between the fiber and the grips of the tensile machine; whereas the fibers extracted from the plasma-sprayed composites were tested with a 25.4 mm gage length after gluing the fibers on cardboard tabs. It should be noted that the data from fibers that failed in the grips during testing at both laboratories were not included in this article.

Scanning electron microscopy was performed on the powder-cloth and plasma-sprayed composites in both the as-fabricated and as-tested conditions. Fracture surfaces of the tested composites were also examined, along with metallographically polished, transverse and longitudinal cross sections of the composites. As-received fibers and extracted fibers were selected for examination by scanning electron microscopy after single-fiber tensile testing was conducted.

III. RESULTS

A. *As-Fabricated Composite Microstructures*

Examples of the fiber distributions in the as-fabricated powder-cloth and plasma-sprayed composites are shown in Figures 1(a) and (b), respectively. It is evident that the fiber spacings in the powder-cloth composites are more irregular, since some fiber movement can occur as the fugitive binders are driven off from the powder cloths during the hot-pressing procedure and later in the process as the matrix material is pressed between the fibers to form a fully consolidated composite. In contrast, the within-ply fiber distribution in the plasma-sprayed composites is more regular, since the matrix material is densely deposited onto the fibers prior to full consolidation of the monotapes. As a result, there is little opportunity for fiber movement to occur during the consolidation process with this fabrication method. The volume fraction of fiber ranged from 23 to 31 vol pct in the powder-cloth composites and from 22 to 24 vol pct in the plasma-sprayed composites. A wider range of

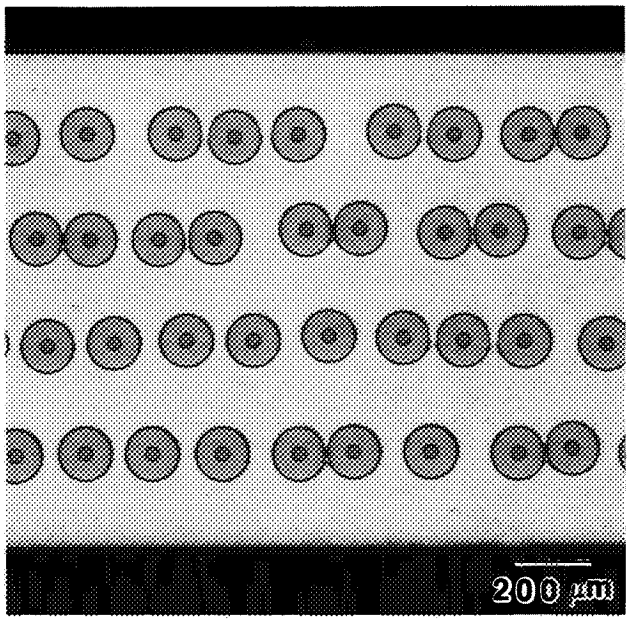

(*a*)

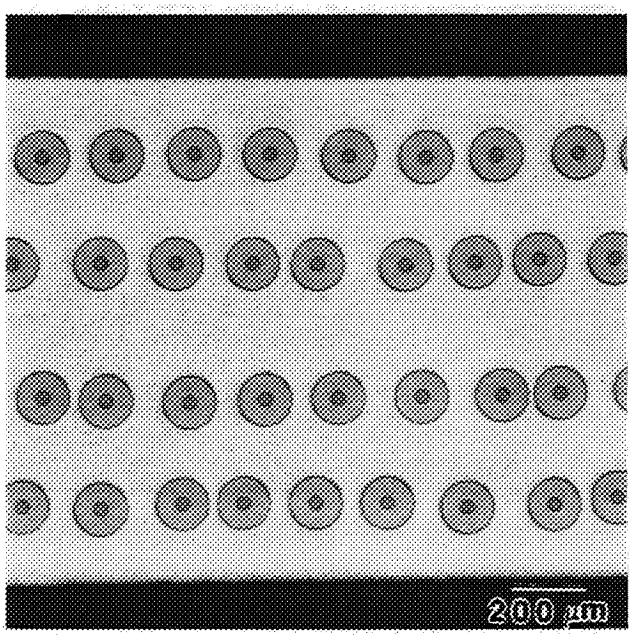

(*b*)

Fig. 1—Typical fiber distributions achieved in as-fabricated, unidirectional SCS-6 SiC/Ti-24Al-11Nb composites fabricated by the (*a*) powder-cloth method and the (*b*) plasma spray technique.

fiber volume fraction was obtained with the powder-cloth method, because the individual powder cloths are rolled manually and precise powder-cloth thicknesses are difficult to achieve.

The as-fabricated microstructures of the powder-cloth and plasma-sprayed composites are shown at higher magnifications in Figures 2(a) through (d), and it is clear that the fabrication methods produce considerable differences. In the powder-cloth material in Figure 2(a), a 2.7 ± 0.08 μm thick carbon-rich coating remains on the SCS-6 fiber after consolidation. A reaction zone is evident between the fiber coating and the matrix, and a uniform β-depleted zone (2 to 10 μm thick) is present in the matrix that is directly adjacent to the reaction zone. The matrix of the powder-cloth composites consists of equiaxed α_2 grains that are surrounded by a discontinuous β phase on the grain boundaries, as seen in Figure 2(c). In contrast, the plasma-sprayed composites have a consistently thinner (2.3 ± 0.16 μm) and more irregular carbon-rich coating on the fiber. Figure 2(b) shows a typical example of the exfoliation of the carbon-rich coating in the plasma-sprayed composites. This exfoliation is caused by the thermal shock that the fibers must withstand as they are sprayed with molten matrix material during fabrication. A multilayered reaction zone forms around each side of the exfoliated fiber coating segments. The β-depleted zone in the plasma-sprayed composites has been observed to range in thickness from about 2 to 40 μm around individual fibers. The irregular thickness of the β-depleted zone appears to have resulted from the inhomogeneous distribution of the β phase in the matrix regions, an example of which is shown in Figure 2(d). The nonhomogeneous distribution of β may be a function of the specific plasma spray parameters used for these panels, since other work[6] has shown that homogeneous microstructures can be produced by plasma spraying.

Table I lists the mean matrix compositions for the starting powder, three of the as-fabricated powder-cloth composite panels, and three of plasma-sprayed panels. The compositions reported are based on duplicate or triplicate measurements. Very good agreement was obtained from these repeat measurements: aluminum and niobium values were within 0.08 at. pct from their respective means; hydrogen and nitrogen values were within 6 ppm from their respective means; and oxygen values were within 35 ppm from their means. Table I indicates that a small amount of aluminum was volatilized during both fabrication methods, whereas the niobium content in the composites was essentially the same as that in the starting matrix powder. In general, the powder-cloth composites had lower amounts of hydrogen, nitrogen, and oxygen pickup compared to the plasma-sprayed material. The fluorine content was determined because a high level of this element is an indication that one of the binders used in the powder-cloth method was not removed; the fluorine content was below the detectability level in all the composites.

B. *Fiber Strengths*

1. *As-received fiber*

Fiber was taken from the spool before and after each drum winding for subsequent tensile testing. This approach enables the as-received fiber strength in each composite panel to be bracketed, and any changes in the strength of the fiber along the spool length can be tracked. Figure 3 displays the mean fiber strength and the 95 pct confidence intervals before and after each drum winding, in the order that the fiber was taken off the spool. The first six data points represent the fiber (25 mm gage length) that was used to fabricate the plasma-sprayed panels, whereas the last four data points

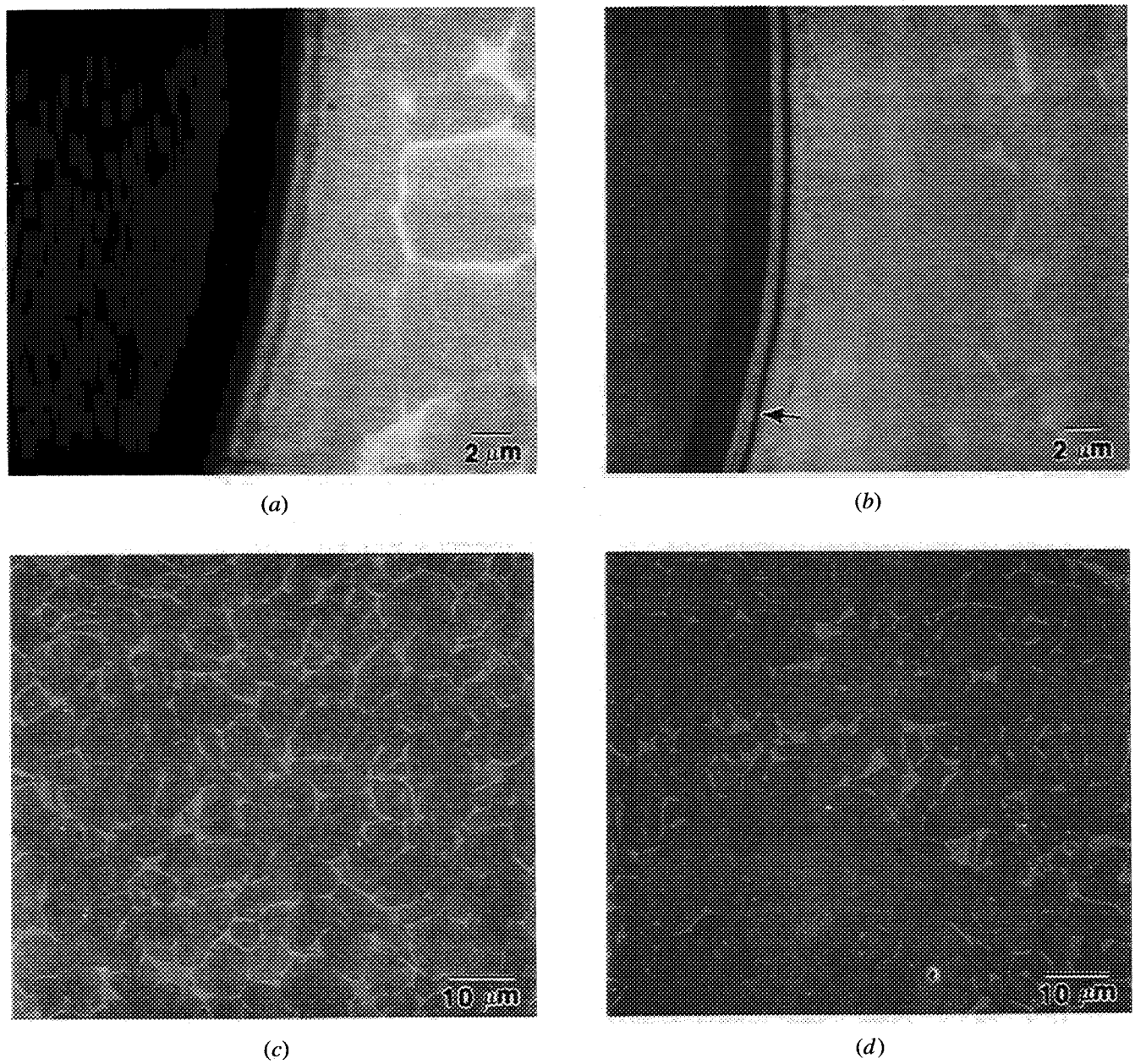

Fig. 2—The microstructure at the fiber-matrix interface is shown for SCS-6 SiC/Ti-24Al-11Nb composites fabricated by the (*a*) powder-cloth method and the (*b*) plasma spray technique. Arrow denotes exfoliation of the carbon-rich fiber coating in (b). The microstructure of the matrix is shown in areas away from the fibers in SCS-6 SiC/Ti-24Al-11Nb composites fabricated by the (*c*) powder-cloth method and the (*d*) plasma spray technique.

represent the fiber (12.7 mm gage length) that was used for the powder-cloth panels. The position along the spool where fiber was taken for each plasma-sprayed and powder-cloth panel is indicated in the figure. It should be noted that the powder-cloth composite panel 91086-4 was fabricated using two fiber mats from each of the first and second powder-cloth fiber windings.

Table II lists the as-received SCS-6 fiber strength data before and after each winding that was used for each composite panel. Figure 3 and Table II show that the biggest change in strength along the spool occurred between positions 3 and 4, which corresponded to before and after the winding that was used for the plasma-sprayed panel RF1716. This large change in strength and the large confidence intervals for the fiber used in the plasma-sprayed panels may be at least partially the result of the smaller number (≤ 10) of single-fiber tests in each data set. The largest change in strength for the fiber used for the powder-cloth panels was between positions 9 and 10, which corresponded to before and after the winding for powder-cloth panel 91086-3. The mean of all the as-received fiber used for the powder-cloth panels was 4577 MPa, and it was 4247 MPa for the plasma-sprayed panels. This 7 pct difference in fiber strength can be accounted for by the difference in gage length used during testing, since the mean strength σ of a fiber is dependent on its gage length L according to the following equation:[11]

Table I. Compositions* of Matrix Powder and of As-Fabricated SiC/Ti-24Al-11Nb (Atomic Percent) Composites

	Al (At. pct)	Nb (At. Pct)	Ti	H (Wt ppm)	N (Wt ppm)	O (Wt ppm)	F (Wt ppm)
Matrix Powder	25.0	10.0	balance	28	88	687	<10
Powder-Cloth Composites**:							
91086-1	23.8	10.2	balance	92	96	1240	<20
91086-2	24.7	10.0	balance	34	96	818	<20
91086-3	24.5	10.0	balance	28	75	845	<20
Plasma-Sprayed Composites**:							
RF1714	23.8	10.1	balance	151	112	1440	<20
RF1715	23.8	10.2	balance	99	100	1340	<20
RF1716	24.8	9.9	balance	33	106	828	<20

*Compositions listed are means obtained from duplicate or triplicate measurements.
**Matrix composition of the composite is reported.

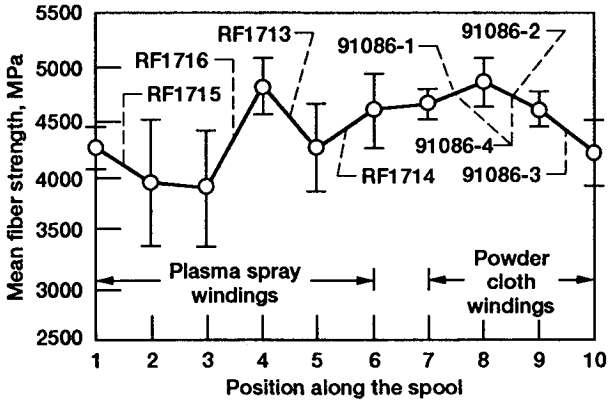

Fig. 3—The means and the 95 pct confidence intervals are given for the as-received SCS-6 fiber strength before and after each drum winding for the plasma-sprayed (gage length = 25 mm) and powder-cloth (gage length = 12.7 mm) composites. The plasma-sprayed and powder-cloth panel numbers are indicated for each drum winding at the mid-points between the mean fiber strengths. The x-axis represents the order in which the fiber was taken off the spool.

$$\sigma_1/\sigma_2 = (L_2/L_1)^{1/m} \quad [1]$$

where m is the Weibull modulus.

The as-received fiber strength data are displayed in the form of a Weibull plot in Figures 4(a) and (b). In these plots, ln ln [1(1 − P)] is displayed as a function of ln stress, where P is the cumulative probability of rupture at a given stress. The straight lines in these figures were determined by least-squares regression. The as-received fibers used for fabricating powder-cloth panels 91086-1, 91086-2, and 91086-4 were not statistically different from one another, so as a result, these data were pooled together for the Weibull distribution in Figure 4(a). As indicated by the open circles in the figure, these fiber strengths could be described well by a single linear regression, the slope of which yielded the Weibull modulus m_1 of 14.7. However, the as-received fibers used for powder-cloth panel 91086-3 were statistically different from those used for the other powder-cloth panels. These data displayed a bimodal distribution and thus were plotted separately in Figure 4(a); these data are represented by the square symbols in the figure. A Weibull modulus m_1 of 24.3 was obtained for the high-strength regime, whereas in the lower strength regime, a slope m_2 of 2.4 was obtained. A similar approach has been used previously[12] for defining an appropriate m_2. The stress range over which each regression was performed is indicated by the extent of the straight lines in the figure.

In contrast, analyses of the as-received fibers used for the plasma-sprayed panels indicated that all panels contained some fibers with strengths under 3600 MPa; bimodal Weibull distributions were consistently displayed by the fibers in each of these panels as well. None of these low fiber strengths came from grip failures during testing; data from fiber tests that failed in the grips were discarded. Since the as-received fiber used to fabricate the four plasma-sprayed panels were not statistically different from one another, all of these data were pooled together for the Weibull plot in Figure 4(b). A bimodal distribution of fiber strength was exhibited by the pooled data. The Weibull modulus m_1 in the high-strength portion of the plot was determined to be 10.6, whereas the slope m_2 in the lower strength region equaled 4.5.

Table III summarizes the as-received fiber strength data for the entire population of fibers in the composite panels, as well as for the high-strength and low-strength regions of the Weibull plots, which are denoted as the m_1 and m_2 regions, respectively. The cumulative probability of rupture P is also given for the transition between the m_1 and m_2 regions; these values indicate the percentage of fibers in the low-strength m_2 region. It should be noted that the number of tests used to determine m_1 and m_2 does not necessarily equal the total number of tests indicated in Table III, because any low fiber strength data points showing large deviations from the m_2 linear region were not included in that regression. It has been suggested that deviations at strengths below the m_2 range may be indicative of a threshold stress,[12] below which the probability of failure is zero.

2. *Extracted fiber*

Fibers were removed from the as-fabricated composite panels by an etching technique in order to investigate any fiber damage that may have been induced during fabrication. The extracted SCS-6 fiber strengths are listed in Table II for individual powder-cloth and

Table II. SCS-6 Fiber Strength for Each Panel*

	Mean (MPa)	Standard Deviation (MPa)	Number of Tests
As-Received fiber:			
For powder-cloth panels:			
before 91086-1	4670	328	23
after 91086-1	4873	476	19
before 91086-2	4873	476	19
after 91086-2	4620	307	17
before 91086-3	4620	307	17
after 91086-3	4236	695	24
before 91086-4**	4762	409	42
after 91086-4**	4754	419	36
For plasma-sprayed panels:			
before RF1713	4829	368	10
after RF1713	4271	518	9
before RF1714	4271	518	9
after RF1714	4605	273	5
before RF1715	4267	267	10
after RF1715	3957	784	10
before RF1716	3912	726	10
after RF1716	4829	368	10
As-received + etched fiber:			
For powder-cloth panel:			
before 91086-1	4810	235	15
Fiber etched from powder-cloth composite panels:			
91086-1	4197	720	21
91086-2	4026	1385	16
91086-3	3790	1287	34
91086-4	4330	1003	11
Fiber etched from plasma-sprayed composite panels:			
RF1713	4260	604	20
RF1714	3881	503	20
RF1715	3743	764	20
RF1716	3876	726	20

*Fiber gage length = 12.7 mm for powder-cloth panels and 25.4 mm for plasma-sprayed panels.

**Panel 91086-4 was fabricated using two fiber mats from each of the first and second powder-cloth fiber windings. Thus, the "before 91086-4" fiber strength data was obtained by pooling the "before 91086-1" and the "before 91086-2" data; the "after 91086-4" fiber strength data was obtained by pooling the "after 91086-1" and the "after 91086-2" data.

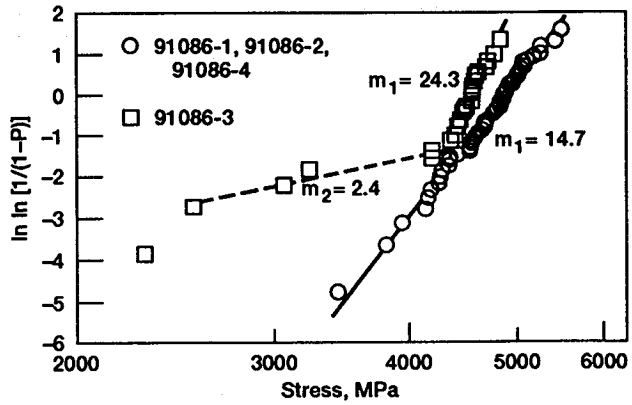

(*a*)

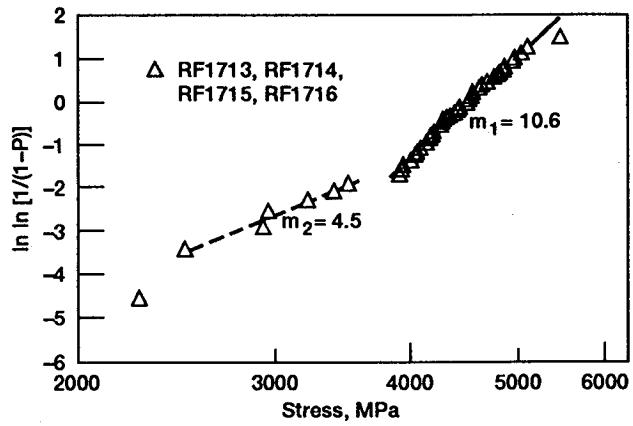

(*b*)

Fig. 4—(*a*) Weibull plot for the as-received fiber used for fabricating the powder-cloth SiC/Ti-24Al-11Nb composites. Circles represent fiber used for panels 91086-1, 91086-2, and 91086-4. Squares represent fiber used for panel 91086-3. (*b*) Weibull plot for the as-received fiber used for all of the plasma spray SiC/Ti-24Al-11Nb composites. The slopes of the high- and low-strength regimes are indicated by m_1 and m_2, respectively.

plasma-sprayed panels, and these data are summarized for each fabrication method in Table III. Figure 5(a) displays the Weibull plot for the as-received and extracted fiber from the powder-cloth panels 91086-1, 91086-2, and 91086-4. Although the as-received data displayed a linear behavior, the extracted fiber data exhibited bimodal behavior. For the extracted fiber data in the high-strength linear region, where most of the data were located, a Weibull modulus of 14.2 was achieved, which was very similar to that obtained for the as-received fiber. About 16 pct of the extracted SCS-6 fibers contributed to the low-strength portion of the curve in Figure 5(a). The fibers in the powder-cloth composites underwent a 12 pct degradation in strength after fabrication, when the means of the combined populations of fiber strengths in Table III were used in the calculation.

As seen in Figure 5(b), the bimodal behavior that was observed for the as-received fiber used in powder-cloth panel 91086-3 persisted after extracting the fiber from that composite panel. The Weibull modulus m_1 dropped from 24.3 to 10.4 after fabrication. This particular panel contained a significantly higher percentage of weak fibers (31 pct) in the m_2 region after fabrication.

Scanning electron microscopy was performed on some of the as-received fibers that were used to fabricate powder-cloth panel 91086-3 and on some of the fibers extracted from that composite panel. The fibers selected for study included both strong and weak fibers; the fracture surfaces of these fibers were examined after single-fiber tensile testing. This examination did not reveal any significant differences between the fracture surfaces of the strong and the weak fibers, nor between those of the as-received and extracted fibers. No flaws were visible either on the fiber surface or internally.

For the plasma-sprayed composites, both the as-received and extracted fiber data displayed a bimodal distribution, as seen in Figure 5(c). The extracted fiber yielded a Weibull modulus m_1 of 7.7 in the high-strength

Table III. SCS-6 Fiber Strength Summary for Composite Fabrication Methods

	Combined Populations				m_1 Region			m_2 Region			m_1 and m_2 Transition
	m	Mean* (MPa)	Standard Deviation (MPa)	Number of Total Tests	m_1	Mean* (MPa)	Number of Tests (for m_1)**	m_2	Mean* (MPa)	Number of Tests (for m_2)**	P (Pct)
As-received fiber:											
For all powder-cloth panels	8.6	4577	538	83	14.3	4694	77	3.5	3069	5	7
For panels 91086-1, 91086-2, 91086-4	14.7	4721	386	59	14.7	4721	59	—	—	0	0
For panel 91086-3	5.6	4236	695	24	24.3	4559	18	2.4	3264	6	23
For all plasma-sprayed panels	7.1	4247	640	49	10.6	4459	42	4.5	2975	6	14
Fiber etched from composite panels:											
From all powder-cloth panels	2.7	4013	1151	82	12.5	4596	60	0.4	2422	6	27
From panels 91086-1, 91086-2, 91086-4	2.7	4170	1030	48	14.2	4592	38	0.9	2567	8	16
From panel 91086-3	2.5	3790	1287	34	10.4	4602	22	0.7	2302	7	31
From all plasma-sprayed panels	6.4	3940	673	80	7.7	4070	74	2.3	2339	5	8

*Fiber testing gage length = 12.7 mm for powder-cloth panels and 25.4 mm for plasma-sprayed panels.
**The number of tests used to calculate m_1 and m_2 does not necessarily add up to the number of total tests, because low fiber strength data points showing large deviations from the m_2 linear region were not included in that regression.

linear region, compared to 10.6 for the as-received data. The m_1 values for the plasma-sprayed composites appeared to be consistently lower than those obtained for the powder-cloth composites. About 8 pct of the extracted fibers contributed to the low-strength m_2 region in Figure 5(c). The fibers in the plasma-sprayed composites exhibited a 7 pct degradation in overall strength after fabrication, when the means of the combined populations of fiber strengths were used in the calculation.

It should be noted that extracted SCS-6 fibers appeared to be particularly sensitive to handling and testing techniques. This is graphically illustrated in Figure 6, which shows two Weibull distributions for fibers extracted from the same four plasma-sprayed panels. Although the fibers were etched from the same composites, the fiber extractions and fiber testing were performed 1 year apart. It is clear from the figure that the data obtained using the "current" technique are very different from those obtained using the "prior" technique. In particular for the prior technique, only 33 pct of the fiber data could be described by the Weibull modulus m_1, compared to 92 pct of the data generated using the current technique. Although differences in techniques of fiber handling and testing are difficult to quantify, it is known that the current techniques at General Electric now employ extra care in preventing touching of the fiber gage lengths during the extraction and tensile testing procedures and in mounting the fibers for tensile testing. Similar cross checks of the NASA procedures have also been performed, and it has been determined that there are no differences between the prior and current testing practices at NASA. Thus, all of the data in Figures 3 through 5 were obtained from adequate extraction and testing techniques that are not believed to influence the results.

C. *Composite Tensile Properties*

Typical tensile stress-strain curves for the powder-cloth and plasma-sprayed unidirectional composites are shown in Figure 7; the solid line represents the powder-cloth tensile curve, and the dotted line represents the tensile curve of the plasma-sprayed composite. The shapes of the curves are characterized by bilinear behavior,[3,13–15] which consists of two linear regions before failure. The first linear region exhibited represents elastic deformation of both the fiber and the matrix;[13] the modulus values listed in Table IV were obtained from this region. The second linear region has been shown to represent elastic deformation of the fiber and the onset of plastic deformation of the matrix.[13,14] The stress at which deviation from linearity first occurs is defined as the elastic limit of the composite and is the stress at which the matrix begins to yield. The strain at the elastic limit occurred around 0.23 pct for the powder-cloth composites and was consistently higher for the plasma-sprayed composites at approximately 0.35 pct.

The longitudinal tensile properties measured for each of the powder-cloth and plasma-sprayed specimens are listed in Table IV. Specimens with reduced gage sections and with rectangular configurations were tested; the properties appeared to be independent of specimen type. The mean elastic modulus for the powder-cloth composites was slightly higher than that for the plasma-sprayed material, since the powder-cloth material had higher fiber volume fractions. The powder-cloth composites had lower elastic limits, which could have resulted from different residual stresses in the composites or from the lower oxygen levels in the matrix. The lower elastic limits in the powder-cloth composites were consistent with the data from the fiberless matrix;[2,16] the powder-cloth matrix was softer than the plasma-sprayed matrix. The mean UTS for the powder-cloth composites was very similar, although slightly higher, to that measured for the plasma-sprayed composites; however, the powder-cloth composites had slightly higher fiber volume fractions. It should also be noted that the standard deviation for the UTS properties was 93.5 MPa for the powder-cloth composites and 78.4 MPa for the plasma-sprayed composites. These standard deviations are the

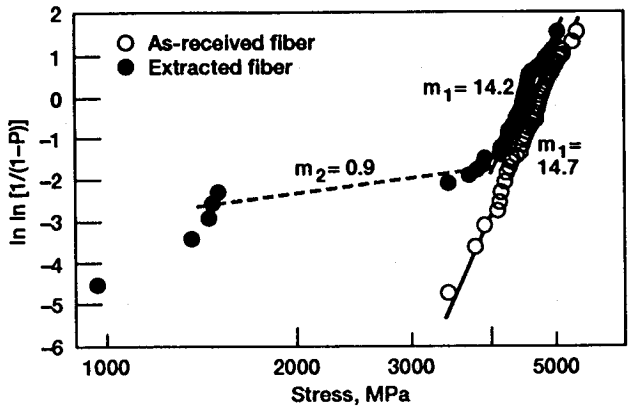

(*a*)

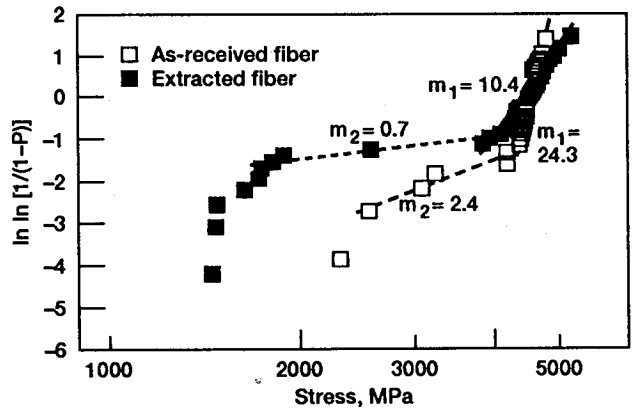

(*b*)

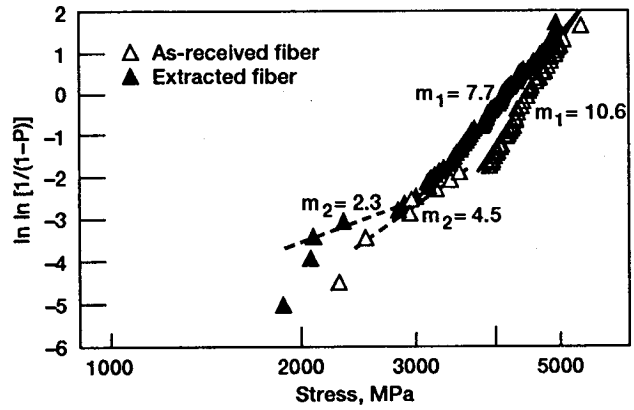

(*c*)

Fig. 5—Weibull plots for the as-received and extracted fiber from: (*a*) powder-cloth panels 91086-1, 91086-2, and 91086-4; (*b*) powder-cloth panel 91086-3; and (*c*) plasma-sprayed panels. Open symbols represent the as-received fiber, and closed symbols represent the extracted fiber. The slopes of the high- and low-strength regimes are indicated by m_1 and m_2, respectively.

same as those reported for composites that had been fabricated with controlled fiber lots[2] and are about 50 pct lower than those observed in composites that had been fabricated with random fiber lots.[2] This is further evidence that variability in composite properties can be reduced when single-fiber lots are used in fabrication.

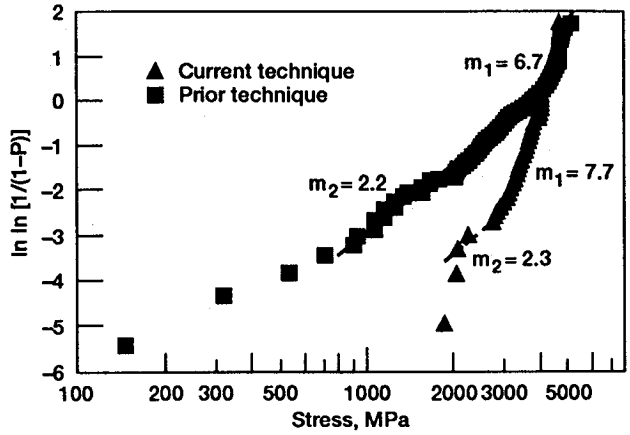

Fig. 6—Weibull plot showing the effect that different handling and testing techniques can have on extracted fiber data from the plasma-sprayed SCS-6 SiC/Ti-24Al-11Nb composites. Triangles represent the data generated with the current techniques, and squares represent the data generated with the prior techniques. The slopes of the high- and low-strength regimes are indicated by m_1 and m_2, respectively.

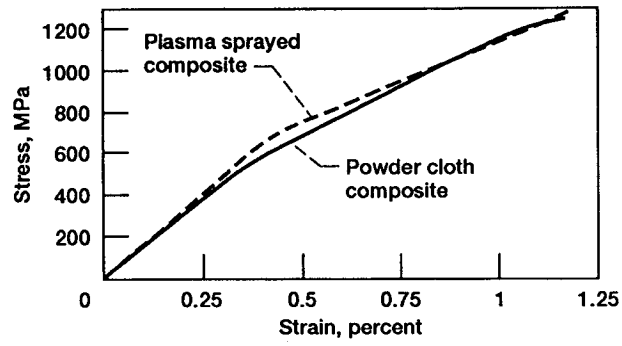

Fig. 7—Typical tensile stress-strain curves generated at room temperature for SCS-6 SiC/Ti-24Al-11Nb composites fabricated by the powder-cloth method (solid line) and the plasma spray technique (dotted line).

Rule of mixtures (ROM) calculations were used to compare the UTS data for each panel, since the volume fraction of fiber varied in these composites. These calculations were determined as follows:

$$\text{ROM UTS} = V_f\sigma_{f,e} + (1 - V_f)\sigma_m, \qquad [2]$$

where V_f is the volume fraction of fiber in the composite panel, $\sigma_{f,e}$ is the mean extracted fiber strength for the composite panel, and σ_m is the strength of the matrix at the failure strain of the composite. It is recognized, however, that the use of a single average fiber strength has limitations, especially in light of the bimodal Weibull distributions shown in Figure 5. The value of σ_m used in this calculation was 574 MPa for the powder-cloth composites[3] and 669 MPa for the plasma-sprayed composites;[16] the matrix strength for the plasma-sprayed material was higher, presumably because of its higher level of oxygen. Both the powder-cloth and the plasma-sprayed composite strengths reached 85 pct of the ROM. This percentage of the ROM is very similar to the

Table IV. Longitudinal Properties of Unidirectional SiC/Ti-24Al-11Nb (Atomic Percent) Composites at Ambient Temperature*

	Panel Number	Specimen Type	Volume Fraction (Pct)	Elastic Limit (MPa)	UTS (MPa)	Strain to Failure (Pct)	Modulus (GPa)
Powder-cloth composites:	91086-1	reduced	23	454	1255	1.09	165
		reduced	24	450	1241	1.17	154
	91086-2	reduced	28	414	1351	1.07	182
		reduced	29	250	1262	1.08	195
	91086-3	reduced	24	488	1227	1.03	171
		reduced	26	226	1089	0.89	191
	91086-4	reduced	31	523	1393	1.08	181
		reduced	27	340	1193	0.93	203
Mean:			26	393	1251	1.04	180
Standard deviation:			2.8	110	93	0.09	16
Plasma-sprayed composites:	RF1713	rectangular	22	597	1234	1.11	163
		rectangular	22	519	1310	1.18	169
		reduced	22	631	1358	1.24	165
		reduced	22	575	1296	1.24	148
	RF1714	rectangular	24	549	1172	1.03	165
		rectangular	24	586	1200	1.04	164
		reduced	24	601	1255	1.11	165
		reduced	23	475	1020	0.98	165
	RF1715	rectangular	22	580	1158	1.00	170
		rectangular	22	619	1227	1.08	165
		reduced	22	561	1213	1.07	166
		reduced	22	571	1172	1.13	146
	RF1716	rectangular	22	530	1227	1.15	161
		rectangular	22	577	1145	1.04	162
		rectangular	22	564	1138	0.99	167
		reduced	22	605	1269	1.18	164
		reduced	24	381	1248	1.23	174
Mean:			23	560	1214	1.11	163
Standard deviation:			1.0	60	78	0.09	7

*All specimen gage lengths = 25.4 mm.

values reported elsewhere[1,2] for SiC/Ti-24Al-11Nb composites.

A more sophisticated model[17] for predicting the UTSs of intermetallic matrix composites was also used. This model is a modified bundle theory that incorporates the statistical nature of fiber strength and accounts for the presence of fiber-matrix sliding and for the load carried by the yielding matrix. The predicted UTS is obtained as follows:[17]

$$\text{UTS} = V_f\left(\frac{2}{m+2}\right)^{1/(m+1)}\left(\frac{m+1}{m+2}\right)\left(\frac{\sigma_{f,e}^m \tau L_0}{r}\right)^{1/(m+1)} + (1 - V_f)\sigma_m \quad [3]$$

where m is the Weibull modulus for the extracted fibers, $\sigma_{f,e}$ is the mean extracted fiber strength for fibers with a gage length L_0, τ is the sliding resistance of the fiber-matrix interface (56 MPa),[3,17] and r is the radius of the SCS-6 fiber. In this study, data for the combined populations of fibers were used for m and $\sigma_{f,e}$. The terms V_f and σ_m have the same definitions as those in Eq. [2]. The powder-cloth composite strengths reached 99 pct of the predicted UTS in Eq. [3], and the plasma-sprayed composites had strengths that reached 91 pct of the predicted value. This good correlation between this modified bundle theory and the experimental results is similar to that reported for other SCS-6/Ti composites.[17]

D. *As-Tested Composite Microstructures*

Longitudinal sections of fractured tensile specimens were polished to the first fiber row for microstructural examination. Multiple fiber cracks were observed in both the powder-cloth and plasma-sprayed composites, and typical examples of this cracking are shown in Figures 8(a) and (b). In general, the majority of the fiber cracks in both the powder-cloth and plasma-sprayed composites were located close to the fracture surface with the frequency of cracking decreasing with increasing distance from the fracture surface. In contrast, the fiber cracks observed previously in tensile-tested powder-cloth composites[2,3] were more periodic in nature and extended farther distances from the fracture surface. In the present study, several specimens from each fabrication method also exhibited large crack-free areas in random locations throughout the longitudinal sections examined. In one specimen from panel RF1714, the majority of the fiber cracks developed along one edge of the composite, and very few fiber cracks were observed in the remainder of the longitudinal section. The nonhomogeneous fiber cracking in this specimen appeared to be correlated to its low-composite tensile strength; this specimen had a UTS of only 1020 MPa.

The number of fiber cracks were counted over a distance of approximately 1 cm from the fracture surface,

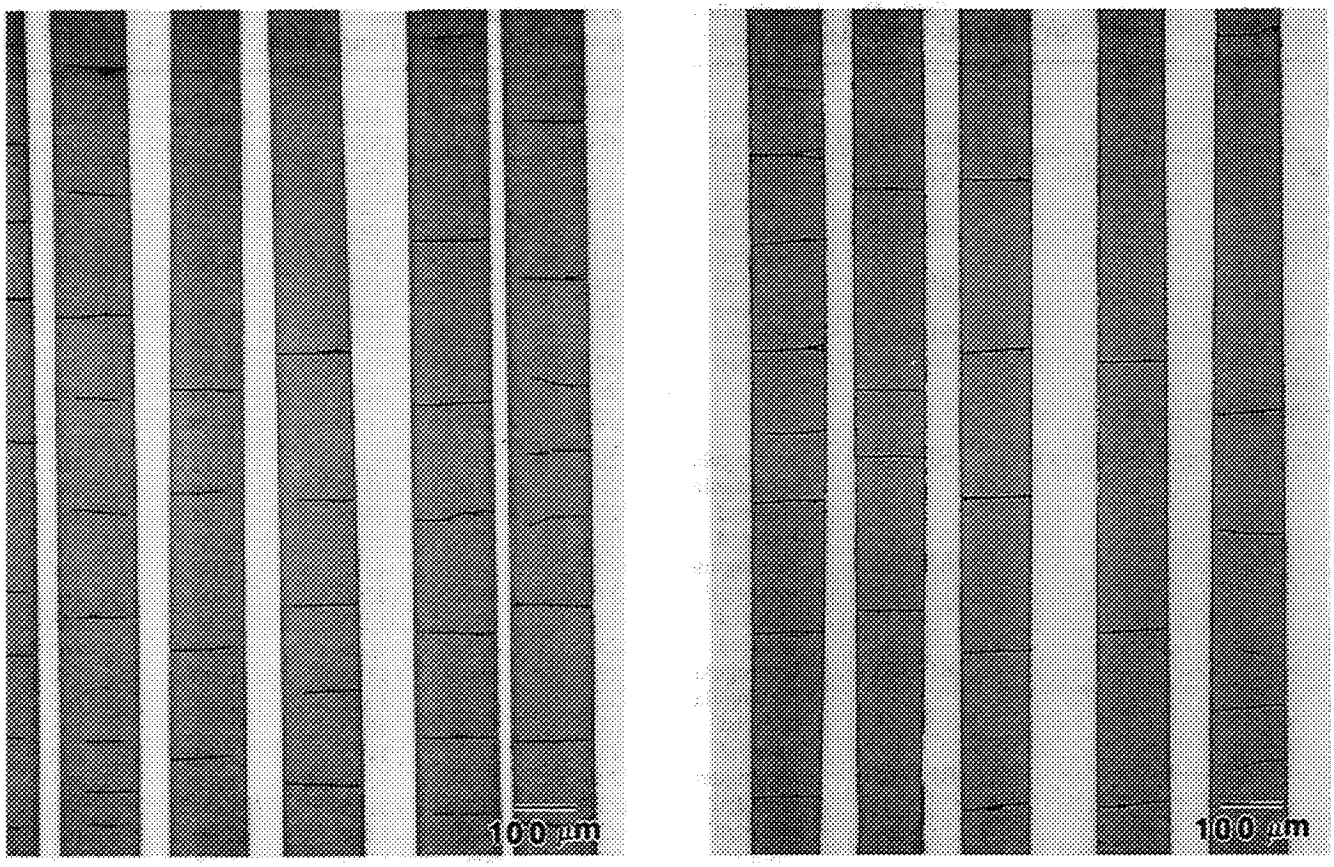

(*a*) (*b*)

Fig. 8—As-tested microstructures showing fiber cracks in SiC/Ti-24Al-11Nb composites fabricated by the (*a*) powder-cloth method and the (*b*) plasma spray technique.

and average crack spacings and standard deviations were calculated. The resulting histograms of the fiber crack spacings for selected powder-cloth and plasma-sprayed composites are shown in Figures 9(a) and (b), respectively. Both the powder-cloth and plasma-sprayed composites had average crack spacings that varied greatly from specimen to specimen, and had large standard deviations as a result of the crack-free areas. A pronounced right-hand tail was also quite evident in many of the crack spacing distributions, again because of the large crack-free areas. However, the positions of the histogram peaks were similar to those in the previous work[18] and ranged from 100 to 200 μm.

In addition to the fiber cracks, axial cracks in the reaction layer and the β-depleted zone were present in both the powder-cloth and plasma-sprayed composites. These axial cracks were generally not associated with the fiber cracks.

The fracture surfaces of the as-tested specimens were examined by scanning electron microscopy, and the percentages of pulled out fibers were obtained for each fracture surface examined. A fiber was considered to be pulled out when the top of the fractured fiber was not coplanar with the surrounding matrix. Typical fiber pullout lengths were approximately 100 to 200 μm. It was found that the fracture surfaces of the powder-cloth and plasma-sprayed composites with similar strengths exhibited similar percentages of pulled out fibers. However, there appeared to be higher percentages of pulled out fibers (~35 pct) in the stronger composite specimens with UTSs greater than 1240 MPa. The weaker composites with strengths under 1175 MPa tended to have lower quantities of fiber pullout (~14 pct), except for powder-cloth composite 91086-3, which again showed anomalous behavior. Panel 91086-3 had 32 pct fiber pullout; it was also the only powder-cloth composite having a bimodal fiber strength distribution in the as-received condition and contained at least twice as many weak fibers in the low-strength m_2 region after fabrication, compared to all of the other composite panels.

IV. DISCUSSION

A lack of linearity in the Weibull distribution plots of fiber strength data has been extensively reported in the literature for ceramic fibers.[12,19–23] It has been suggested that this nonlinear behavior is indicative of a complex or multimodal flaw distribution.[20,22] Much of the SCS-6 fiber tested in the present study displayed nonlinear Weibull distributions with shapes that were very similar to that observed in another recent study[19] for SCS-6 fiber strengths after extraction from an orthorhombic titanium matrix. The nonlinear Weibull distribution reported previously has been interpreted[19] as resulting

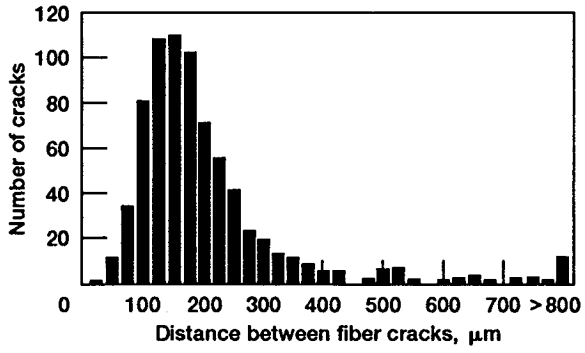

(*a*)

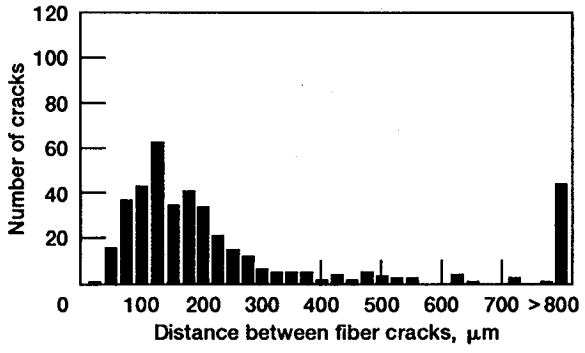

(*b*)

Fig. 9—Histograms displaying the frequency of fiber cracking in the outer plys of as-tested SiC/Ti-24Al-11Nb composites fabricated by the (*a*) powder-cloth method and the (*b*) plasma spray technique.

from fibers that were damaged either during composite fabrication or fiber extraction, which introduced a new population of flaws. In contrast, another study[2] has shown that as-received SCS-6 fiber and SCS-6 fiber extracted from a Ti-24Al-11Nb powder-cloth matrix can produce single-mode Weibull distributions.

It is well recognized that ceramic fibers are extremely sensitive to handling and testing methods, as evidenced by the data in Figure 6. However, the fiber used for the powder-cloth composites was tested in the same manner as that in Reference 2, and thus the Weibull distributions shown in Figures 4 and 5 are not the result of poor handling or inadequate testing methods. Since as-received fibers were placed in the etchant used for fiber removal, and no difference in mean strength was measured, as seen in Table II, the fiber extraction procedure did not appear to contribute to the fiber degradation, which is also in agreement with previous results.[2] Therefore, it is more likely that the bimodal Weibull distributions for the as-received and extracted fiber data in the present study are due to the nature of the particular lot of SCS-6 fiber used. Scanning electron microscopy, however, did not reveal any flaws or features that could have contributed to the bimodal fiber distributions. No flaws were visible on the fracture surfaces of as-received fibers or fibers extracted from powder-cloth composites after single-fiber tensile testing. It is possible that some portion of the fiber fracture surface was lost during tensile testing because of the shattering of the fiber that often occurs during failure. However, it is clear that this particular lot of fiber was more susceptible to fabrication damage, since other lots of SCS-6 fiber have been used to fabricate composites by the nominally same powder-cloth method. In these earlier studies,[2] no bimodal Weibull distributions of fiber strength were obtained in either the as-received condition or after fabrication, and only a 4 pct degradation in fiber strength was observed after powder-cloth fabrication.

The increased sensitivity of the particular fiber lot selected for this investigation is further supported by composite panel 91086-3; this panel contained the only as-received fiber for the powder-cloth material that displayed a bimodal distribution with 23 pct of the fibers contributing to the low-strength m_2 region. The nonlinear behavior of the Weibull distribution persisted after extraction from the composite, and 31 pct of the fibers contained in the composite contributed to the low-strength m_2 region. Panel 91086-3 was clearly the weakest of the powder-cloth composite panels, and the as-received fiber that was used to fabricate that particular panel appeared to contribute to its lower tensile strength. This observation is in agreement with previous work,[2] which concluded that the strength of composites intentionally fabricated with 67 pct high-strength fiber and 33 pct lower strength fiber was dominated by the lower strength fiber.

In the present study, the amount of fiber strength degradation appeared to be similar after fabrication by either method: a 12 pct degradation in fiber strength was observed after powder-cloth fabrication, and a 7 pct degradation strength was observed after plasma spraying when the overall means for the combined populations were used in the calculation. It is recognized that because of the bimodal Weibull distributions in Figure 5, using a single value of extracted fiber strength represents an oversimplification in calculating the percentage of fiber strength degradation. However, the fiber degradation values for the powder-cloth composites do appear to be higher in this study than in a previous one,[2] which reported only a 4 pct degradation after fabrication and extraction from the powder-cloth composites. The degradation of the fibers after extraction from HIPed plasma-sprayed panels is less than that observed in an earlier investigation,[5] where a 25 pct degradation in fiber strength was reported. It is suspected by the present authors, however, that fabrication and testing methods have evolved and have been improved since the work in Reference 5 was performed; thus, the 25 pct strength degradation reported may no longer be accurate.

The plasma-sprayed fibers might be expected to have lower strengths because of the exfoliation of the carbon-rich coating, and because the carbon-rich coating was thinner as a result of the additional reaction with the matrix during consolidation. However, this was not demonstrated in the present study. It appears that this outer fiber coating acts as a sacrificial layer, and as long as the SiC portion of the fiber remains protected, the fiber does not lose any additional strength relative to the degradation induced by other fabrication methods. This is consistent with a study[24] conducted on panels that had been fabricated using a large number of different lots of

SCS-6 fiber; it was found that significant losses in post-consolidation fiber strength did not occur until the average thickness of the remaining carbon-rich coating was <2 μm. Exfoliation of the carbon-rich coating also appeared to have little impact on longitudinal tensile properties of the composite, since longitudinal sections of the tested composites did not show any preferential cracking at these fiber coating defects. However, it is possible that exfoliation may adversely affect off-axis composite properties and long-term composite properties, where the fiber-matrix interface becomes more influential.

The powder-cloth and plasma spray fabrication methods provided composites with similar longitudinal tensile properties at room temperature. Despite the fiber coating exfoliation and the differences in the matrix microstructure, the fiber-matrix interface, and the fiber distribution between the two types of composites, the properties appear to be controlled primarily by the strength of the fibers. As in previous studies,[1,2] the ROM was not reached by the composites when the means of the combined populations of extracted fiber strengths were used in the calculation. The modified bundle theory did provide an improvement over the ROM in the prediction of the composite UTS. However, the good agreement between the UTS predicted from the modified bundle theory and the experimentally measured UTS may be somewhat fortuitous, since Eq. [3] was derived for fibers displaying single-mode Weibull distributions. The lot of fibers used in the present study is believed to have two populations of flaws, and hence, use of a single mean fiber strength in either the ROM or the modified bundle theory is an oversimplification.

Earlier work[2] confirmed that 33, 67, or 100 pct lower strength fibers were each sufficient to dominate the tensile behavior of the composite and lower its strength. Since the composites in this study contained between 8 and 31 pct low-strength fibers, fiber data from the m_2 region were inputted into Eqs. [2] and [3] to determine if better agreement between theory and experiment would ensue. However, use of the m_2 data resulted in an underestimation of the composite UTS by up to 20 pct. Therefore, it appears that these models require further development for the prediction of composite strengths, especially when the composites contain fibers with bimodal Weibull distributions. It was also noted in earlier work[2] that the SCS-6 fibers in Ti-24Al-11Nb composites actually failed at lower stresses compared to single-fiber tests, which may mean that the properties obtained from single-fiber tests may not be precisely equal to those *in situ*. This may provide a further complication when predictions of composite properties are made.

The fiber cracks and the fracture surfaces of the failed specimens indicated that most of the composites were failing by a mixture of cumulative and noncumulative damage. Cumulative damage occurs when the weakest fibers crack in a random manner and the load transfers to the neighboring fibers which remain intact; noncumulative damage occurs when only a few weak fibers fail and cause final fracture to propagate across the remaining load-bearing cross section of the composite. Cumulative damage was apparent in all of the specimens because of the existence of multiple fiber cracks away from the fracture surface. The fracture surfaces of the higher strength composites also showed evidence of cumulative damage because of the increased quantities of fiber pullout, which is consistent with fibers fracturing randomly throughout the specimen. However, noncumulative damage was also apparent in all of the composite specimens because of the increased density of fiber cracks and axial cracks in the fiber-matrix interfaces near the fracture surface. The lower strength composites tended to have highly localized regions containing a multitude of cracking which probably provided sufficient stress concentrations such that other fibers in their vicinity failed prematurely. The fracture surfaces of these lower strength composites exhibited a small amount of fiber pullout, which is consistent with a noncumulative fracture mode.

V. CONCLUSIONS

1. Very similar longitudinal tensile properties were exhibited by composites fabricated by the powder-cloth and plasma spray methods when the starting fiber and matrix constituents were controlled and effectively equivalent. This suggests that similar levels of fiber damage occurred in both types of composites during fabrication.
2. The standard deviations of the composite strengths were lower than for those composites in previous studies that were fabricated using random fiber lots. This provides further evidence that the variability in composite properties can be reduced when single-fiber lots are used in fabrication.
3. The particular lot of SCS-6 fiber selected for this study was more susceptible to damage during composite fabrication than those used in previous studies, since the fiber strengths obtained in this study tended to exhibit bimodal Weibull distributions, with a larger percentage of weak fibers present after fabrication.
4. Microstructural differences in the composites as a result of different fabrication methods did not appear to impact fiber-controlled longitudinal properties at least on a first-order basis. However, these differences may become more influential in off-axis or long-term properties where the fiber-matrix interface, the fiber distribution, and the matrix microstructure may play a larger role.

ACKNOWLEDGMENTS

The authors would like to express their appreciation to Drs. M.V. Nathal and J.A. DiCarlo for insightful technical discussions; A. Veverka, D. Revlock, and J. Juhas for powder-cloth processing; S. Rutkowski for plasma spraying; and M. McQuater, W. Karpinski, P. Dupree, and S. Weaver for fiber and composites testing.

REFERENCES

1. R.A. MacKay, P.K. Brindley, and F.H. Froes: *JOM*, 1991, vol. 23, pp. 23-29.
2. S.L. Draper, P.K. Brindley, and M.V. Nathal: *Metall. Trans. A*, 1992, vol. 23A, pp. 2541-48.

3. P.K. Brindley, S.L. Draper, J.I. Eldridge, M.V. Nathal, and S.M. Arnold: *Metall. Trans. A*, 1992, vol. 23A, pp. 2527-40.
4. J.M. Larsen, K.A. Williams, S.J. Balsone, and M.A. Stucke: in *High Temperature Aluminides and Intermetallics*, S.H. Whang, C.T. Liu, D.P. Pope, and J.O. Stiegler, eds., TMS-AIME, Warrendale, PA, 1990, pp. 521-56.
5. H. Gigerenzer and P.K. Wright: in *Titanium Aluminide Composites*, P.R. Smith, S.J. Balsone, and T. Nicholas, eds., WL-TR-91-4020, Wright Patterson Air Force Base, Dayton, OH, Feb. 1991, pp. 251-64.
6. D.R. Pank, A.M. Ritter, R.A. Amato, and J.J. Jackson: in *Titanium Aluminide Composites*, P.R. Smith, S.J. Balsone, and T. Nicholas, eds., WL-TR-91-4020, Wright Patterson Air Force Base, Dayton, OH, Feb. 1991, pp. 382-98.
7. J.W. Pickens, J.W. Smith, and B.A. Lerch: in *NASA CP 10104*, vol. II, NASA-Lewis Research Center, Cleveland, OH, 1992, pp. 31-1-31-17.
8. J.W. Pickens, R.D. Noebe, G.K. Watson, P.K. Brindley, and S.L. Draper: *NASA TM-102060*, NASA-Lewis Research Center, Cleveland, OH, 1989.
9. P.A. Siemers and J.J. Jackson: in *Titanium Aluminide Composites*, P.R. Smith, S.J. Balsone, and T. Nicholas, eds., WL-TR-91-4020, Wright Patterson Air Force Base, Dayton, OH, Feb. 1991, pp. 233-51.
10. F.E. Wawner: in *Fiber Reinforcements for Composite Materials*, A.R. Bunsell, ed., New York, NY, Elsevier, 1988, pp. 371-425.
11. S. van der Zwaag: *J. Test. Eval.*, 1989, vol. 17, pp. 292-98.
12. E. Bourgain and J.J. Masson: *Compos. Sci. Technol.*, 1992, vol. 43, pp. 221-28.
13. B.A. Lerch: *NASA TM-103760*, NASA-Lewis Research Center, Cleveland, OH, 1991.
14. R.P. Nimmer, P.A. Siemers, M.R. Eggleston, and E.S. Russell: in *Titanium Aluminide Composites*, P.R. Smith, S.J. Balsone, and T. Nicholas, eds., WL-TR-91-4020, Wright Patterson Air Force Base, Dayton, OH, Feb. 1991, pp. 596-619.
15. S. Jansson, H.E. Deve, and A.G. Evans: *Metall. Trans. A*, 1991, vol. 22A, pp. 2975-84.
16. A.M. Ritter, F.C. Clark, and P.L. Dupree: in *Light-Weight Alloys for Aerospace Applications II*, E.W. Lee and N.J. Kim, eds., TMS-AIME, Warrendale, PA, 1991, pp. 403-12.
17. W.A. Curtin: *Composites*, 1993, vol. 24, pp. 98-102.
18. S.L. Draper, P.K. Brindley, and M.V. Nathal: Paper presented at 1992 TMS-AIME Annual Spring Meeting, San Diego, CA, March 1–5, 1992.
19. J.R. Porter: in *Intermetallic Matrix Composites II*, D.B. Miracle, D.L. Anton, and J.A. Graves, eds., Materials Research Society, Pittsburgh, PA, 1992, vol. 273, pp. 315-24.
20. P. Martineau, M. Lahaye, R. Pailler, R. Naslain, M. Couzi, and F. Cruege: *J. Mater. Sci.*, vol. 19, 1984, pp. 2731-48.
21. K. Goda and H. Fukunaga: *J. Mater. Sci.*, vol. 21, 1986, pp. 4475-80.
22. K.K. Phani: *J. Am. Ceram. Soc.*, vol. 70 (8), 1987, pp. C-182-C-184.
23. H.F. Wu and A.N. Netravali: *J. Mater. Sci.*, vol. 27, 1992, pp. 3318-24.
24. A.M. Ritter and P.L. Dupree: *Scripta Metall.*, 1992, vol. 27, pp. 827-31.